Zeitschrift für Kristallographie 148, 237–253 (1978)

Thermal change in unit-cell dimensions, and a hexagonal structure of tridymite

Kuniaki Kihara

Department of Earth Sciences, Faculty of Science, Kanazawa University, Kanazawa 920, Japan

Received: July 28, 1978

Abstract. Monoclinic tridymite from a fired silica brick was found to transform to a hexagonal structure at about 420° C on the basis of the measurements of cell dimensions and the integrated intensities as functions of temperature. This tridymite changes its structure on increasing temperature; below 100° C it is monoclinic; 100 to 160° C, orthorhombic II; 160 to 420° C, orthorhombic I, and above 420° C it is in the hexagonal form.

The structure of the hexagonal form, which was refined from Gibbs' structure with space group $P6_3/mmc$ by use of X-ray intensity data measured at 460° C, has 0.0620(4) for the z coordinate of the silicon atom. Thermal vibrations for the oxygen atoms were too large and strongly anisotropic; an alternative model, in which oxygen atoms are located on the circumferences of circles normal to Si–Si lines is also presented. This model gave mean bond lengths Si–O = 1.607 and O–O = 2.63 Å, and mean angles Si–O–Si = 149.2 and O–Si–O = 109.5°.

Introduction

Monoclinic tridymite is known to occur in terrestrial rocks, lunar rocks, meteorites and synthetic materials. Tridymite from the Steinbach meteorite was found to be monoclinic at room temperature and to be transformed into an orthorhombic structure at about 180° C (Dollase and Buerger, 1966; Dollase, 1967). Recently it was found that monoclinic tridymite from fired silica brick is transformed into an

another orthorhombic structure at about 105° C, before the appearence of the orthorhombic form at 180° C (Kihara, 1977). In this study, to distinguish the two orthorhombic phases, the lower-temperature form is termed orthorhombic II (abbreviated O II), and the higher-temperature form, orthorhombic I (O I). Above room temperature, this tridymite from silica brick is transformed with increasing temperature succesively in the order: monoclinic, O II, O I and probably hexagonal form. Nukui et al. (1978) found in X-ray and optical studies on synthetic tridymite that the transition between the O I and hexagonal form occurs at 380° C.

The general features of the hexagonal structure were given by Gibbs (1927). At a temperature well above its transition point the structure has space group $P6_3/mmc$ with cell dimensions $a = 5.03$ and $c = 8.22$ Å. Sato (1964) reported good agreement between powder-diffraction intensities measured on natural and synthetic tridymite at 500° C and those calculated on the basis of the Gibbs' structure, where z_{Si} was 1/16.

Dollase (1967) determined the structure of the O I form at 220° C, which was termed orthorhombic high tridymite and was noted to continue to exist above 250° C. In this structure in space group $C222_1$ six-membered rings of silica tetrahedra have nearly hexagonal shape, but the tetrahedra are rotated around the two-fold axes parallel to a from their positions in the hexagonal structure.

The monoclinic structure with space group Cc was independently determined by Dollase and Baur (1976), and Kato and Nukui (1976). The former authors pointed out that the six-membered rings are distorted into two different configurations; two thirds have a ditrigonal shape and one third have an oval shape in any tridymite layer, where ditrigonal rings may stack above ditrigonal rings or above oval rings and vice versa.

The structure of the O II form has a $3 \times 1 \times 1$ cell compared to that of the O I form. In this structure with space group $P2_12_12_1$ the six-membered rings are distorted in a way similar to those of the monoclinic form and the same ring types stack on top of one another along the orthorhombic c axis (Kihara, 1977). The O II form does not appear in the Steinbach tridymite, which gives reflections corresponding to the O I form, accompanied by satellite reflections in the pseudohexagonal a^* direction between 107 and 180° C. The separation of the satellites varies continuously from that corresponding to about 105 Å at 107° C to about 65 Å at 180° C (Dollase, 1967).

In this paper the thermal-expa
the hexagonal form are discusse
single crystals.

Specimens and equipment

X-ray diffraction experiments w
PW1100 four-circle diffractomete
mated by a flat graphite crystal,
cases, specimens were heated wit
spherical shape having a diamete
was fixed at a position above c
imately 0.5 mm. Temperatures
thermocouple.

The crystal used were from
Messrs. T. Ono and K. Sak
Laboratory. In these experiment
and A # 13 were used; these crys
than 2×10^{-3} mm^3. In the scan
employing an energy-dispersion
dication of impurity in some fra
monoclinic tridymite are usually
expression for the twin relation i
take one of six possible orientati
around $[103]_m$ (Hoffmann, 1967

Through repeated heating
between the monoclinic and O II
untwinned crystal can be transfo
crystal by a continuous rise of te
is maintained or oscillated aroun
to the O II region, the crystal is
relation for diffraction purposes
three orientations rotated by
orthorhombic c direction. For
Kihara (1977) observed that
appears with the a and b directi

[1] In this study the monoclinic form
Aa, the cell constants of which are abo
This is obtained from Hoffmann's set

In this paper the thermal-expansion behavior and the structure of the hexagonal form are discussed on the basis of X-ray data from single crystals.

Specimens and equipment

X-ray diffraction experiments were carried out by use of a Philips PW1100 four-circle diffractometer, using Mo$K\alpha$ radiation monochromated by a flat graphite crystal, and the precession method; in both cases, specimens were heated with the aid of an electric furnaces of spherical shape having a diameter of about 10 mm. A thermocouple was fixed at a position above crystal; the separation was approximately 0.5 mm. Temperatures given in this study are those of the thermocouple.

The crystal used were from refractory silica brick provided by Messrs. T. Ono and K. Sakai, of the Asahi Glass Research Laboratory. In these experiments, three specimens $A\,\#\,11$, $A\,\#\,12$ and $A\,\#\,13$ were used; these crystals had nearly equal volume of less than $2\times10^{-3}\,\mathrm{mm}^3$. In the scanning electron-microscopic analysis employing an energy-dispersion X-ray detector, there was no indication of impurity in some fragments of this tridymite. Crystals of monoclinic tridymite are usually twinned. For diffraction purposes an expression for the twin relation is as follows: each component[1] may take one of six possible orientations rotated by 60° from each other around $[103]_m$ (Hoffmann, 1967).

Through repeated heating experiments across the transition between the monoclinic and O II forms, it was found that a monoclinic untwinned crystal can be transformed to an orthorhombic untwinned crystal by a continuous rise of temperature but, when the temperature is maintained or oscillated around the transition point and then raised to the O II region, the crystal is easily twinned. In this case the twin relation for diffraction purposes is that each component takes one of three orientations rotated by 120° from each other around the orthorhombic c direction. For the specimen from fired silica brick, Kihara (1977) observed that at this transition the new structure appears with the a and b directions rotated by 60° (or 120°) around

[1] In this study the monoclinic form is represented by a unit-cell with space group Aa, the cell constants of which are about $a = 25.8$, $b = 5.0$, $c = 18.5$ and $\beta = 117.7°$. This is obtained from Hoffmann's setting by a transformation $(001/0\bar{1}0/100)$.

monoclinic c^* from the positions of the corresponding monoclinic axes. After that, the crystal was repeatedly heated and cooled across the transition point. The relation held even then, but not when the temperature was oscillated in a small range ($\approx 10°$) around the transition point. Precession photographs taken under such conditions showed reciprocal-lattice patterns in which the O II form was found to be twinned by components in two orientations. Recently Nukui et al. (1978) showed that a single crystal of synthetic monoclinic tridymite was transformed into the O II form twinned by components in six (effectively three) orientations rotated by 60° from each other around c. These observations indicate that, at this transition the monoclinic structure can go to the O II structure in one or more orientations.

The unit-cell dimensions were measured mainly using crystal $A \# 11$ and $A \# 13$, which are both twinned. The crystal $A \# 11$ was twinned by components in two orientations rotated by 180° from each other. The volume ratio was estimated as 0.9 : 0.1 below the transition point (about 100° C). On the other hand, the twin ratio in $A \# 13$ was estimated above the transition point. In this case two of the three orientations were predominant, the ratio being 0.64 : 0.36.

Thermal expansion

Each reciprocal-lattice constant was determined by the diffractometer, employing the centers of gravity of reflections along the corresponding rows through the origin in the range $\theta = 3-20°$. For example, the $h00$, $0k0$ and $00l$ rows and, in the case of the monoclinic form, in addition, the $h0h$ row, were independently used for a^*, b^*, c^* and β^*. Crystal $A \# 11$ was used for both the monoclinic and the O II form, and $A \# 13$ for both the O I and the hexagonal form.

A major error may be caused by use of overlapped reflections. From many X-ray experiments with tridymite it is believed, however, that overlapping is nearly perfect for the twinning in the monoclinic form. Taking account of both this and the fact that one orientation was predominant in $A \# 11$, reflections available in the procedure were all used in the determination of the reciprocal-lattice constants of the monoclinic form. In the range of both orthorhombic forms, measurements for $0k0$ reflections gave relatively large errors, which probably originated from imperfect overlapping. In the precession photographs of the O II form, splitting of some reflections was observed when twinning had occurred. For the O I form, the error in

b^* became small with increasing t
would be an indication of distortion c
one in the hexagonal structure, it is su
that the distortion is significant in th
a higher-temperature region in the
these circumstances only the 020 and
of the orthorhombic forms. Except i
points most measurements were carı
one heating cycle.

In Figure 1 the thermal expansion
as functions of temperature [where
cell of the monoclinic form as fc
$B = b_m$ $(= b_{\mathrm{OII}} = b_{\mathrm{OI}})$ and $C = d$
Two abrupt changes correspond
monoclinic and the O II forms and be
respectively. The transition points
temperatures than presented in Kih
used was not twinned. In the O II fo
the B and C directions, although ex
compared to the structure of the m
value of $A/3\,B$ of this structure is
observed region. The value of A is nea
between the O II and the O I form, w
increase with increasing temperatu
respectively. The expansion coefficie
seen to decrease in B with increasin
420° C in C suggests that a transition
which no remarkable change is dete
are nearly constant. The ratio $A/3\,B$
departure from this value is undete

Hexagonal tridymite

Symmetry and transition temperatu

In order to examine the Friedel symm
temperature region, integrated inte
a hemisphere of $\theta = 20°$ were meas
Crystals $A \# 12$ and $A \# 13$, which
these measurements. As a result

b^* became small with increasing temperature. Since the splitting would be an indication of distortion of the cell from the corresponding one in the hexagonal structure, it is suggested from these observations that the distortion is significant in the O II form and becomes small in a higher-temperature region in the O I form. Consequently under these circumstances only the 020 and $0\bar{2}0$ reflections were used for b^* of the orthorhombic forms. Except in the proximity of the transition points most measurements were carried out at given temperatures in one heating cycle.

In Figure 1 the thermal expansions of A, B, C and $A/3\,B$ are shown as functions of temperature [where A, B and C are normalized to the cell of the monoclinic form as follows: $A = a_m$ $(= a_{\mathrm{OII}} = 3\,a_{\mathrm{OI}})$, $B = b_m$ $(= b_{\mathrm{OII}} = b_{\mathrm{OI}})$ and $C = d(001)_m$ $(= 2\,c_{\mathrm{OII}} = 2\,c_{\mathrm{OI}} = 2\,c_h)$]. Two abrupt changes correspond to the transitions between the monoclinic and the O II forms and between the O II and the O I forms, respectively. The transition points are seen to be shifted to lower temperatures than presented in Kihara (1977), in which the crystal used was not twinned. In the O II form the structure is contracted in the B and C directions, although expanded in the A direction, when compared to the structure of the monoclinic form. As the result the value of $A/3\,B$ of this structure is most deviated from $1/\sqrt{3}$ in the observed region. The value of A is nearly constant above the transition between the O II and the O I form, while those of B and C continue to increase with increasing temperature up to about 340 and 420° C, respectively. The expansion coefficient is seen to increase in C, though seen to decrease in B with increasing temperature. A bend at about 420° C in C suggests that a transition occurs at this temperature, above which no remarkable change is detected and the unit-cell dimensions are nearly constant. The ratio $A/3\,B$ gradually approachs to $1/\sqrt{3}$; the departure from this value is undetectable at 340° C.

Hexagonal tridymite

Symmetry and transition temperature

In order to examine the Friedel symmetry for the structure in a higher-temperature region, integrated intensities of observable reflections in a hemisphere of $\theta = 20°$ were measured at 380, 400, 420 and 460° C. Crystals A # 12 and A # 13, which are both twinned, were used for these measurements. As a result, both crytals showed intensity

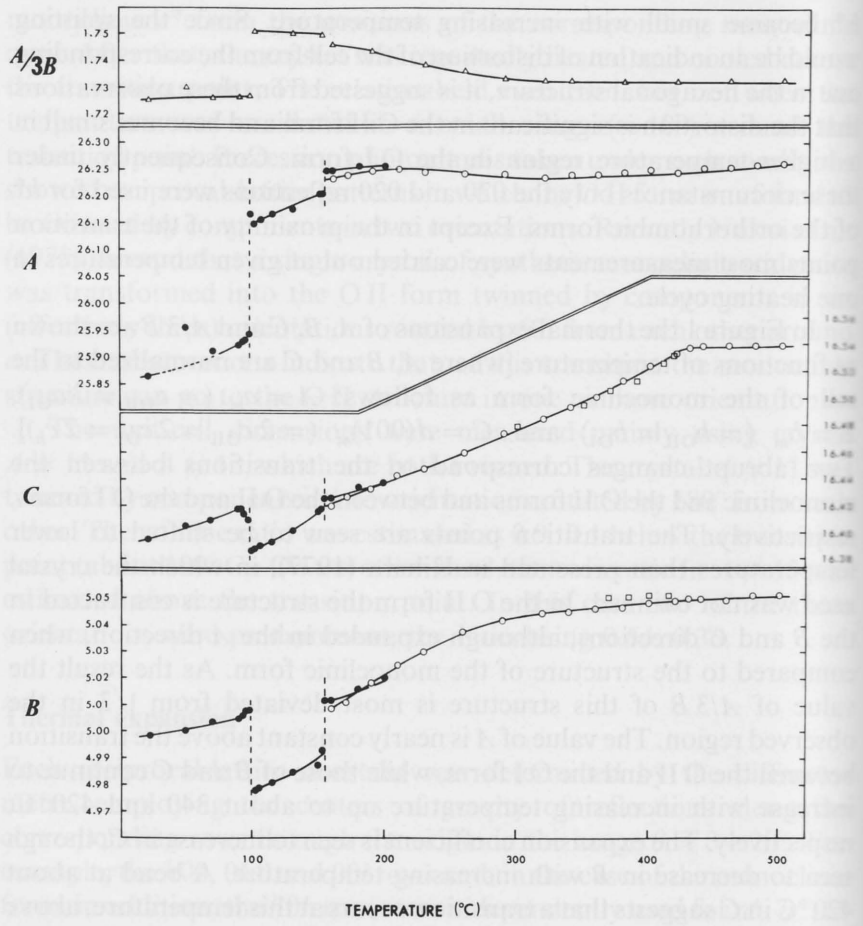

Fig. 1. Thermal expansion behavior in three orthogonal directions for three crystals: white circles for A # 13, black circles for A # 11 and squares for A # 12. A, B and C are respectively chosen to correspond to the a, b, and d (001) of the cell of the monoclinic form

distributions having nearly hexagonal symmetry $6/mmm$ at the temperatures examined. At 300° C some pairs of reflections with relatively weak intensities were seen to violate orthorhombic symmetry. Intensities of such pairs of reflections were measured as a function of temperature; the result showed that intensity differences observed in each pair gradually decreased and were almost undetectable at 380° C (Fig. 2).

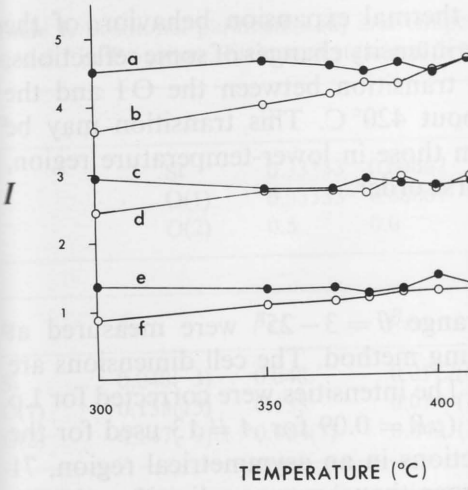

Fig. 2. Integrated intensities (arbitrary scale) o for O I region; a: $\bar{3}30$, b: 330, c: $\bar{1}30$, d: 130,

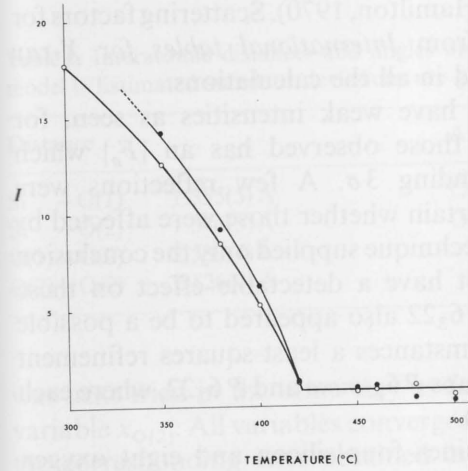

Fig. 3. Changes of integrated intensities (ar reflections 621 (white circles) and $\bar{6}21$ (black

Through these intensity measure pairs of reflections the intensities de range up to about 420° C. Figure 3 sh of the integrated intensities of r correspond respectively to 221 and

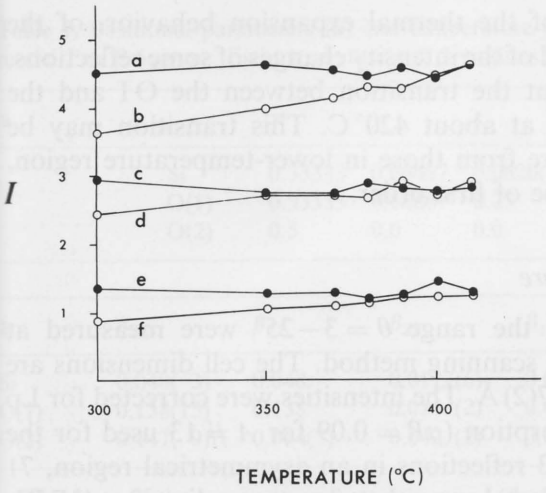

Fig. 2. Integrated intensities (arbitrary scale) of some reflections measured on A # 12 for O I region; a: $\bar{3}30$, b: 330, c: $\bar{1}30$, d: 130, e: $\bar{3}32$ and f: 332

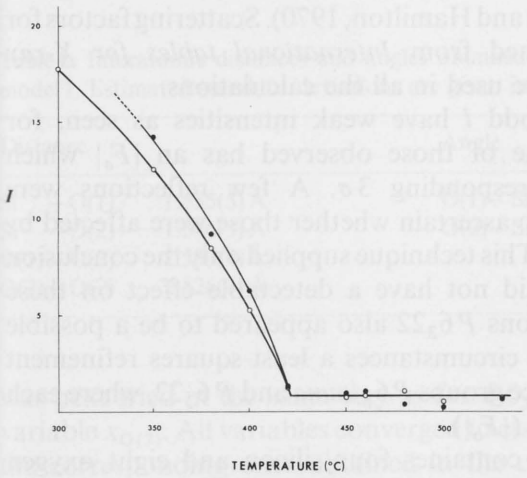

Fig. 3. Changes of integrated intensities (arbitrary scale) with temperature of the reflections 621 (white circles) and $\bar{6}21$ (black circles)

Through these intensity measurements, it was found that for some pairs of reflections the intensities decrease rapidly in the temperature range up to about 420° C. Figure 3 shows the temperature dependence of the integrated intensities of reflections 621 and $\bar{6}21$, which correspond respectively to 221 and $42\bar{1}$ for the hexagonal structure.

From observations of the thermal expansion behavior, of the intensity distribution, and of the intensity changes of some reflections, it may be concluded that the transition between the O I and the hexagonal forms occurs at about 420° C. This transition may be distinguished in its nature from those in lower-temperature region, which are both seen to be of first order.

Refinement of the structure

Integrated intensities in the range $\theta = 3-25°$ were measured at 460° C, using the $\omega-2\theta$ scanning method. The cell dimensions are $a = 5.052(9)$ and $c = 8.27(2)$ Å. The intensities were corrected for Lp factors, but not for absorption ($\mu R = 0.09$ for $A \# 13$ used for the measurements). Of all 93 reflections in an asymmetrical region, 71 reflections whose $|F_o|$'s are larger than corresponding 2σ ($|F_o|$)'s (where σ is standard deviation estimated from counting statistics) were used for least-squares refinement. This was carried out using the program LINUS (Coppens and Hamilton, 1970). Scattering factors for half-ionized atoms obtained from *International tables for X-ray crystallography* (1974) were used in all the calculations.

Reflections *hhl* with odd *l* have weak intensities as seen, for example, in Figure 3. One of those observed has an $|F_o|$ which approximates to the corresponding 3σ. A few reflections were examined by ψ scanning to ascertain whether those were affected by multiple scattering or not. This technique supplied only the conclusion that multiple scattering did not have a detectable effect on these reflections. For these reasons $P6_322$ also appeared to be a possible space group. Under these circumstances a least-squares refinement was first tried for both space groups $P6_3/mmc$ and $P6_322$, where each $|F_o|$ was weighted by $1/\sigma^2$ ($|F_o|$).

A hexagonal unit-cell containes four silicon and eight oxygen atoms, which were initially assigned to three sets of special positions in the two space groups. Four silicon atoms were assigned to equipoint 4*f*, two oxygen atoms to 2*c* and six oxygen atoms to 6*g*. This structure corresponds to that given by Gibbs (1927) and tentatively termed model I.

Refinement based on $P6_3/mmc$ with variable parameters z_{Si}, anisotropic temperature parameters, and an isotropic extinction parameter, gave an *R* value of 0.067 and a weighted $R = (\Sigma\omega|\Delta F|^2/\Sigma\omega|F_o|^2)^{\frac{1}{2}}$ of 0.061 for the 71 reflections. Refinement based on $P6_322$

Table 1. Positional parameters (**a**) and tempe model I in $P6_3/mmc$. Estimated standard dev

a		*x*	*y*
	Si	0.33333	0.66667
	O(1)	0.33333	0.66667
	O(2)	0.5	0.0

b	β_{11}	β_{22}	β_{33}
Si	0.048(3)	0.048	0.0117(
O(1)	0.138(15)	0.138	0.014 (
O(2)	0.147(9)	0.064(7)	0.042 (

The form of the temperature factors is exp $+ 2\beta_{13}hl + 2\beta_{23}kl)$

Table 2. Interatomic distances and angles ob model I. Estimated standard deviations are gi

Distance		A
Si –O(1)	1.555(5) Å	O
Si –O(2)	1.546(3) Å	O
O(1)–O(2)	2.530(4) Å	
O(2)–O(2)	2.526(4) Å	

was next tried in the same way as fo variable $x_{O(2)}$. All variables converge the corresponding ones obtained in $= 0.066$ and weighted $R = 0.060$. T converged to 0.526(20), which large both parameters are erroneously dete suggest that $P6_3/mmc$ is not rejected parameters are given in Table 1 fo $P6_3/mmc$. The interatomic distance root mean squared amplitudes and t the thermal ellipsoids to the crys Table 3.

Table 1. Positional parameters (**a**) and temperature parameters (**b**), as refined on model I in $P6_3/mmc$. Estimated standard deviations are given in parentheses

a		x	y	z	B
	Si	0.33333	0.66667	0.0620(4)	3.4 Å^2
	O(1)	0.33333	0.66667	0.25	8.2 Å^2
	O(2)	0.5	0.0	0.0	9.6 Å^2

b	β_{11}	β_{22}	β_{33}	β_{12}	β_{13}	β_{23}
Si	0.048(3)	0.048	0.0117(6)	0.024	0.0	0.0
O(1)	0.138(15)	0.138	0.014 (2)	0.069	0.0	0.0
O(2)	0.147(9)	0.064(7)	0.042 (2)	0.032	0.013	0.026(4)

The form of the temperature factors is exp $-(\beta_{11}h^2 + \beta_{22}k^2 + \beta_{33}l^2 + 2\beta_{12}hk + 2\beta_{13}hl + 2\beta_{23}kl)$

Table 2. Interatomic distances and angles obtained from the refinement based on model I. Estimated standard deviations are given in parentheses

Distance		Angle	
Si $-$O(1)	1.555(5) Å	O(1)$-$Si$-$O(2)	109.4(2)°
Si $-$O(2)	1.546(3) Å	O(2)$-$Si$-$O(2)	109.6(2)°
O(1)$-$O(2)	2.530(4) Å		
O(2)$-$O(2)	2.526(4) Å		

was next tried in the same way as for $P6_3/mmc$ with the additional variable $x_{O(2)}$. All variables converged to essentially the same values as the corresponding ones obtained in the case of $P6_3/mmc$, with $R = 0.066$ and weighted $R = 0.060$. The relaxed oxygen x parameter converged to 0.526(20), which largely correlates with β_{11} and thus both parameters are erroneously determined. In any event these points suggest that $P6_3/mmc$ is not rejected. The positional and temperature parameters are given in Table 1 for the final refinement based on $P6_3/mmc$. The interatomic distances and angles are given in Table 2; root mean squared amplitudes and the relation of the principal axes of the thermal ellipsoids to the crystallographic axes are shown in Table 3.

Table 3. Root mean squared amplitudes along the principal axes of the thermal ellipsoids obtained from the refinement for model I. The orientations of the ellipsoids are given with respect to the [210], b and c directions

		Root mean squared amplitude	[210]	b	c
Si	1	0.21 Å			90.0°
	3	0.20			0.0
O(1)	1	0.36			90.0
	3	0.22			0.0
O(2)	1	0.41	30.0°	120.0°	90.0°
	2	0.20	62.9	37.8	114.2
	3	0.40	78.2	69.2	24.2

The thermal motion as refined here is only slightly larger in magnitude than in the O I form of the Steinbach tridymite (Dollase, 1967): using a quantity $\langle u^2 \rangle$ defined as $\frac{1}{3}(\langle u_1^2 \rangle + \langle u_2^2 \rangle + \langle u_3^2 \rangle)$ for convenience' sake, the mean values are 0.042 and 0.040 Å^2 for silicon, and 0.117 and 0.106 Å^2 for oxygen in the hexagonal and the O I form, respectively. On the other hand, the values for these structural states are apparently larger than those in the lower-temperature forms: $\langle u(\mathrm{Si})^2 \rangle = 0.010$ and $\langle u(\mathrm{O})^2 \rangle = 0.025$ Å^2 for the monoclinic form (calculated from Kato and Nukui, 1976) and 0.030 and 0.067 Å^2 for the O II form (Kihara, 1977). Although an allowance should be made for the different sources of the specimens used in these studies, it can be concluded that the thermal motions of atoms in the O I structure and in this hexagonal structure refined on the model I are not so much different from each other.

The silicon ellipsoid is nearly spherical, but the oxygen ellipsoids have oblate spheroidal shapes; the shortest axis is in the Si–Si line and the other two are normal to it. The ellipsoid of the O(2) atom is apparently larger and more anisotropic than that of the O(1) atom. It should be noted that the oxygen ellipsoids are circular in the hexagonal form, but not so in the O I form of the Steinbach tridymite, around the Si–Si lines; the magnitude along the shortest axes is apparently smaller in the hexagonal form.

In the refinements of high cristobalite (Peacor, 1973; Leadbetter et al., 1973), the oxygen atoms were refined to six positions being equally

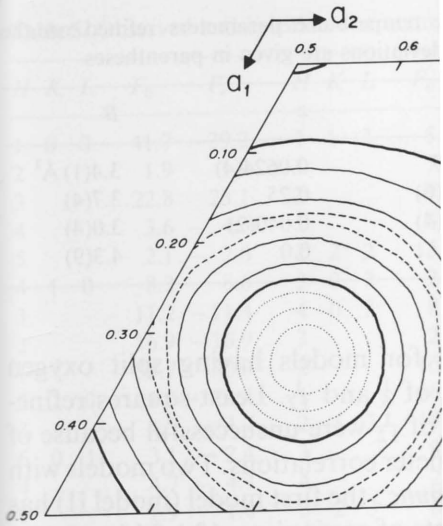

Fig. 4. Difference-Fourier section at $z = \frac{1}{4}$ position of O(1) is at the center of circles. Co zero contours: dotted lines indicate nega positive contours of value 0.5 e

spaced around a circle perpendicula of atoms have B factors which are n in magnitude: $B(\mathrm{Si}) \approx 3.5$ and $B($

The root mean squared amplitu model I (Table 3) are seen to be t thermal vibration alone. In a differe isotropic temperature parameters l and their neighborhoods show ne rounded by positive and circular lines. From this difference map, it m are located around the circumferer some positions, probably six for expected that the strongly anisotr atoms may be interpreted by takin cristobalite structure with respec models in which each of the mean on the respective circumferences m such models require unreasonab tetrahedra.

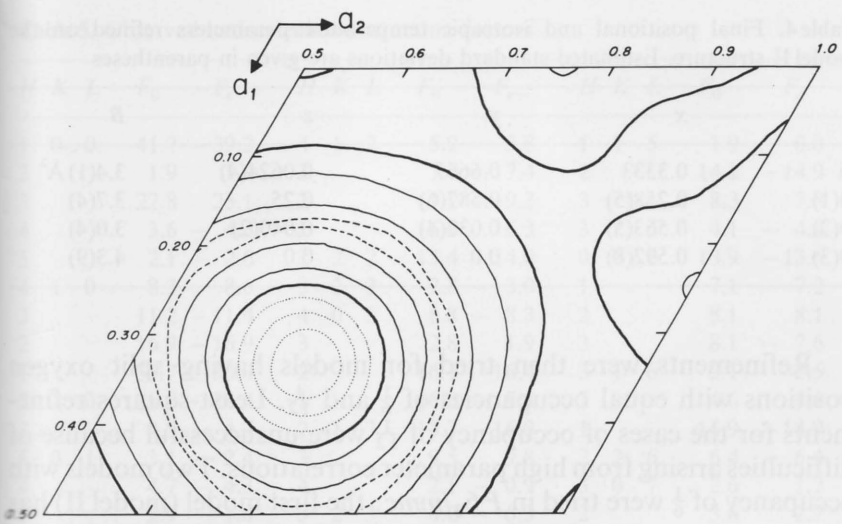

Fig. 4. Difference-Fourier section at $z = \frac{1}{4}$ of the hexagonal structure. The mean position of O(1) is at the center of circles. Contour interval is 0.2 e; thick lines indicate zero contours: dotted lines indicate negative contours and dashed lines indicate positive contours of value 0.5 e

spaced around a circle perpendicular to the Si – Si lines and both kinds of atoms have B factors which are not much different from each other in magnitude: $B(\mathrm{Si}) \approx 3.5$ and $B(\mathrm{O}) \approx 3.9\,\text{Å}^2$ at 300° C.

The root mean squared amplitudes of the oxygen atoms refined in model I (Table 3) are seen to be too large for those to result from thermal vibration alone. In a difference-Fourier map (Fig. 4) based on isotropic temperature parameters listed in Table 1 b, all atom centers and their neighborhoods show negative distributions and are surrounded by positive and circular distribution normal to the Si – Si lines. From this difference map, it may be suggested that oxygen atoms are located around the circumferences of the circles and localized to some positions, probably six for respective Si – Si lines. It is thus expected that the strongly anisotropic and large ellipsoids of oxygen atoms may be interpreted by taking models, for example, like the high-cristobalite structure with respect to oxygen positions. Structure models in which each of the mean oxygen positions is split into three on the respective circumferences may be rejected because it seems that such models require unreasonably large distortion of the silica tetrahedra.

Table 4. Final positional and isotropic temperature parameters refined on the model II structure. Estimated standard deviations are given in parentheses

	x	y	z	B
Si	0.3333	0.6667	0.0624(4)	3.4(1) Å^2
O(1)	0.258(5)	0.587(6)	0.25	3.7(4)
O(2)	0.563(5)	0.037(4)	0.040(2)	3.0(4)
O(3)	0.592(8)	0.0	0.0	4.3(9)

Refinements were then tried for models having split oxygen positions with equal occupancies of $\frac{1}{6}$ and $\frac{1}{12}$. Least-squares refinements for the cases of occupancy of $\frac{1}{12}$ were unsuccessful because of difficulties arising from high parameter correlations. Two models with occupancy of $\frac{1}{6}$ were tried in $P6_3/mmc$: the first model (model II) has oxygen atoms assigned to three sets of equipoints, 12*j*, 24*l* and 12*i*, and the second model (model III) has four sets of oxygen atoms, 6*h*, 6*h*, 12*k* and 24*l*. Model II may be useful in explaining the difference map and in the other model the oxygen atoms were located in positions rotated by about 30° from those in model II. Agreement between $|F_o|$'s and $|F_c|$'s better than $R = 0.21$ was not given by the latter. On the contrary, refinement based on model II gave $R = 0.053$ and weighted $R = 0.051$, where a scale factor, four B factors, an isotropic extinction parameter and seven positional parameters were refined. Model II was next refined in $P6_322$, but a significant improvement of the R value was not given and the estimated standard deviation of each parameter is as large or equal of the corresponding parameter in $P6_3/mmc$. The positional and temperature parameters are given for the case of $P6_3/mmc$ in Table 4 and the observed and calculated structure factors are listed in Table 5. The interatomic distances and angles are shown in Table 6. An attempt to refine the β_{ij}'s indicated that β_{33}'s of O(2) and O(3) largely correlate with each other and with $z_{O(2)}$. Additional cycles were separately carried out on the β_{ij}'s and on the positional parameters. The improvement of R value was not seen to be significant.

In all the refinements described above it was found that the reflections with conditions $h-k = 3n$ and $l = 2n + 1$ have observed structure factors larger than the calculated ones, although the intensities are so weak that most $|F_o|$'s are not greater than corresponding σ's. This kind of systematic difference between $|F_o|$'s and

Table 5. Observed and calculated

H	K	L	F_0	F_c	H	K
1	0	0	41.7	−39.2	4	1
2			1.9	1.9	3	
3			22.8	23.1	2	
4			3.6	− 4.3	1	
5			2.1	− 2.6	2	2
4	1	0	8.3	8.6	3	2
3			11.2	−11.4	4	0
2			16.9	−16.9	3	
1			30.7	30.0	2	
2	2	0	21.5	22.4	1	
3			4.5	− 4.7	2	1
5	0	1	3.1	2.4	3	
4			4.7	− 4.3	4	
3			2.9	1.0	3	2
2			15.2	14.9	0	0
1			23.4	−22.8	1	
2	1	1	10.4	−11.2	2	
3			5.1	5.4	4	
3	2	1	3.4	− 3.0	2	1
0	0	2	50.3	53.0	2	2
1			16.4	−16.4	3	
2			8.4	8.5	4	0
3			12.5	12.5	2	
4			2.7	− 2.5	1	

$|F_c|$'s is more clearly seen in
by Dollase (1967), but n
monoclinic forms. Althoug
effects, e.g., anharmonic n
bution to the intensities
regarding these effects is n

Taking account of the s
noted above, the presenc
$P6_3/mmc$ does not necess
structure is not $P6_3/mmc$.

Description of the model I

In the model II structure
tetrahedron. They are loc

Table 5. Observed and calculated structure factors

H	*K*	*L*	F_0	F_c	*H*	*K*	*L*	F_0	F_c	*H*	*K*	*L*	F_0	F_c
1	0	0	41.7	−39.2	4	1	2	5.9	5.8	1	1	5	1.9	0.0
2			1.9	1.9	3			7.7	− 7.4	2			14.2	−14.9
3			22.8	23.1	2			9.2	− 9.3	3			8.3	7.8
4			3.6	− 4.3	1			6.0	6.3	3	2	5	4.1	− 4.4
5			2.1	− 2.6	2	2	2	13.4	14.0	0	0	6	13.9	−13.6
4	1	0	8.3	8.6	3	2	2	2.8	− 3.0	1			7.1	7.2
3			11.2	−11.4	4	0	3	8.8	− 8.3	2			8.1	8.1
2			16.9	−16.9	3			2.8	1.9	3			8.1	− 7.6
1			30.7	30.0	2			16.1	16.4	3	1	6	2.1	2.5
2	2	0	21.5	22.4	1			16.0	−15.8	2			4.6	4.6
3			4.5	− 4.7	2	1	3	15.7	−16.0	1			14.9	−14.9
5	0	1	3.1	2.4	3			9.5	9.8	2	2	6	6.4	− 6.4
4			4.7	− 4.3	4			2.1	− 0.9	3	0	7	2.6	1.2
3			2.9	1.0	3	2	3	6.2	− 6.3	2			3.6	2.7
2			15.2	14.9	0	0	4	25.1	24.7	2	1	7	3.7	− 3.5
1			23.4	−22.8	1			7.2	− 7.2	3			2.6	1.6
2	1	1	10.4	−11.2	2			5.9	5.7	0	0	8	10.1	− 9.8
3			5.1	5.4	4			1.9	0.8	1			4.9	4.8
3	2	1	3.4	− 3.0	2	1	4	3.4	− 2.2	2			3.0	3.3
0	0	2	50.3	53.0	2	2	4	2.4	2.3	3			5.6	− 5.4
1			16.4	−16.4	3			2.0	0.5	2	1	8	3.4	3.6
2			8.4	8.5	4	0	5	6.5	− 6.3	1			9.0	− 8.3
3			12.5	12.5	2			17.2	17.1	2	0	9	2.1	− 1.5
4			2.7	− 2.5	1			20.8	−20.5					

$|F_c|$'s is more clearly seen in the result for the orthorhombic form given by Dollase (1967), but not clearly in the cases of the O II and monoclinic forms. Although it may be suggested that some additional effects, e.g., anharmonic motion of atoms, make important contribution to the intensities of these reflections, a further account regarding these effects is not given in this study.

Taking account of the systematically larger $|F_o|$'s of the reflections noted above, the presence of the reflections apparently violating $P6_3/mmc$ does not necessarily imply that the space group of this structure is not $P6_3/mmc$.

Description of the model II structure

In the model II structure there are 24 oxygen positions for each tetrahedron. They are located on a circle for O(1) atoms and three

Table 6. The Si – O and O – O distances and the O – Si – O and Si – O – Si angles for a tetrahedron (Fig. 5) in model II

Distance		Angle	
Si – O(1)	1.600(6) Å	Si – O(2) – Si	149(2)°
O(2)	1.648(14)	O(2)	149(2)
O(3)	1.615(12)	O(3)	147(2)
O(2)	1.564(16)	O(1)	152(2)
mean	1.607	mean	149.2
O(1) – O(2)	2.63(3)	O(1) – Si – O(2)	110(1)
O(1) – O(2)	2.59(2)	O(2) – Si – O(3)	107(2)
O(1) – O(3)	2.66(3)	O(1) – Si – O(2)	108(1)
O(2) – O(3)	2.58(5)	O(2) – Si – O(3)	108(2)
O(3) – O(2)	2.62(6)	O(2) – Si – O(2)	112(2)
O(2) – O(2)	2.67(3)	O(1) – Si – O(3)	112(2)
mean	2.63	mean	109.5

slightly prolate circles for O(2) and O(3) atoms normal to the Si – Si lines. The O(1), O(2) and O(3) atoms are shifted by 0.39, 0.43 and 0.46 Å respectively from the Si – Si lines. The smallest circle, on which the O(1) atoms are located, leads to a c dimension slightly longer than that expected by assuming the regular tetrahedron located on the mean positions (model I); the value of c/a is 1.637 for the observations above 430° C and 1.633 for the calculation.

Probable combinations for the tetrahedron were chosen based on the distances and angles calculated for all atom pairs in a tetrahedron. A combination is shown in Figure 5. The tetrahedron has two O – O distances of 2.66 and 2.67 Å and four in the range 2.58 – 2.63 Å which give two O – Si – O angles of 112° and four in the range 107 – 110°. Hence the mode of distortion of the tetrahedron is very similar to that in the high-cristobalite structure (Peacor, 1973). The Si – O distances are in the range 1.564 – 1.648 Å with a mean value of 1.607 Å, and the Si – O – Si angles are in the range of 147 – 152° with a mean value of 149°. All the values noted here are close to those in the monoclinic structure, and they fall in a range similar to that in the monoclinic form. The isotropic B factors are 3.4 Å^2 for silicon and in the range of 3.0 – 4.3 Å^2 for oxygen atoms.

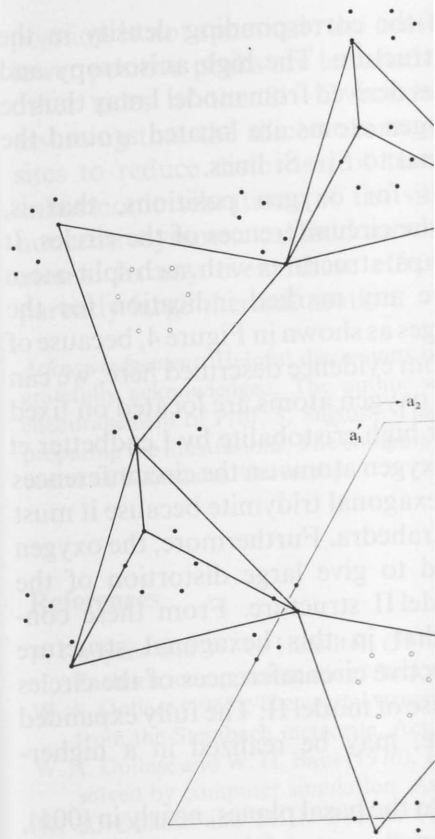

Fig. 5. The hexagonal structure of mod
circles indicate the positions of oxygen

Discussion

The refinement based on mode
consistent with those establi
Comparing the refinements ba
suggested that the improvement
would be significant. On the oth
calculated for model I with a
(Table 1), the centers and the
negative and surrounded by posi
the isotropic temperature facto
model II, the positive distributio

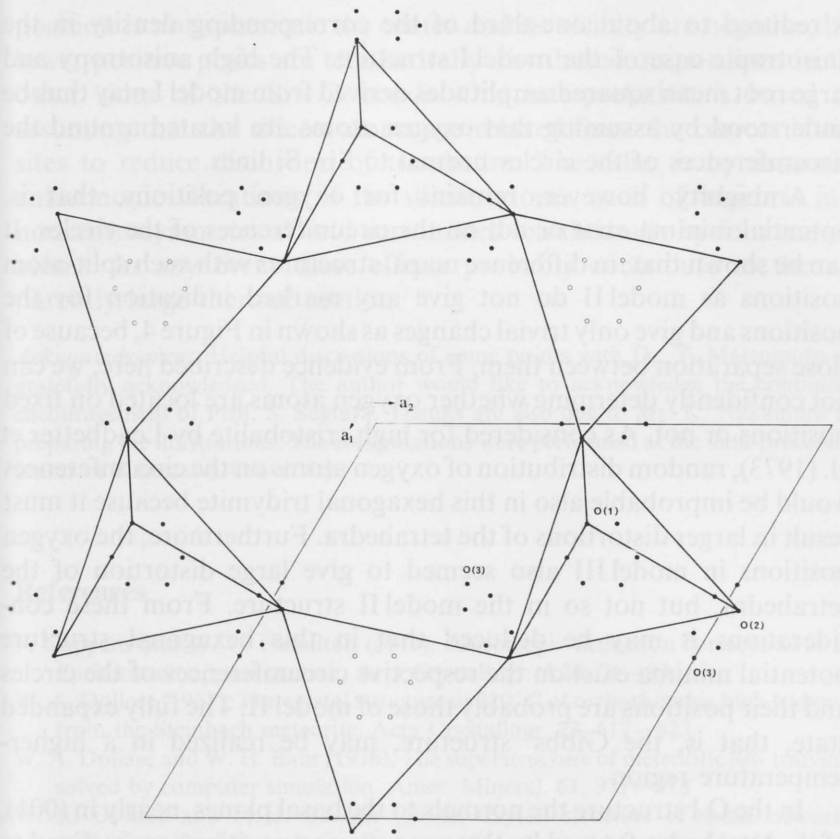

Fig. 5. The hexagonal structure of model II, projected on (0001). White and black circles indicate the positions of oxygen atoms

Discussion

The refinement based on model II gives bond lengths and angles consistent with those established for other silica structures. Comparing the refinements based on both model I and II, it is suggested that the improvement of the R value given by the latter would be significant. On the other hand, in a difference-Fourier map calculated for model I with anisotropic temperature coefficients (Table 1), the centers and the neighborhood of oxygen atoms are negative and surrounded by positive circular density as in the case for the isotropic temperature factors. On the contrary, in the case of model II, the positive distribution disappears and the negative height

is reduced to about one-third of the corresponding density in the anisotropic case of the model I structure. The high anisotropy and large root mean squared amplitudes derived from model I may thus be understood by assuming that oxygen atoms are located around the circumferences of the circles normal to Si–Si lines.

Ambiguity, however, remains for oxygen positions, that is, potential minima exist or not on the circumferences of the circles. It can be shown that, in difference maps, structures with such split-atom positions as model II do not give any marked indication for the positions and give only trivial changes as shown in Figure 4, because of close separation between them. From evidence described here, we can not confidently determine whether oxygen atoms are located on fixed positions or not. As considered for high cristobalite by Leadbetter et al. (1973), random distribution of oxygen atoms on the circumferences would be improbable also in this hexagonal tridymite because it must result in larger distortions of the tetrahedra. Furthermore, the oxygen positions in model III also seemed to give large distortion of the tetrahedra, but not so in the model II structure. From these considerations it may be deduced that in this hexagonal structure potential minima exist on the respective circumferences of the circles and their positions are probably those of model II. The fully expanded state, that is, the Gibbs' structure, may be realized in a higher-temperature region.

In the O I structure the normals to the basal planes, nearly in (001), of the tetrahedra formed by the mean oxygen positions are inclined to the c direction. The c dimension is estimated by using this angle, ϕ, on the basis of a relation $c = 4h \cos\phi$, where h is the corresponding height of the tetrahedron. Furthermore, since the departure of the x coordinates of the mean oxygen positions from those in the hexagonal structure is very small, b is also expressed as $b \approx 2d \cos\phi$, where d is the edge length of the tetrahedron close to the b direction. If the shape of the tetrahedron formed by the mean oxygen positions and the ratio among the apparent root mean squared amplitudes of oxygen atoms are kept unaltered in the region of the O I form, both relations must give approximately equal expansion coefficients in both directions. Accordingly, inconsistent expansion behavior in these directions (Fig. 1) would be explained by considering their changes.

The thermal ellipsoid of the silicon atom refined for this hexagonal structure is nearly spherical and large, i.e., $B(\mathrm{Si}) = 3.4\,\text{Å}^2$. It is suggested from the difference map that distribution around the silicon

position is not spherical: the cen
lower positive peaks are tetrahed
other sides of the Si–O bond
assuming that the silicon atoms
sites to reduce distortion of tet
anharmonic vibrations of the s
noncentrosymmetrical field surr
atoms. In any event these effe
parently large thermal motion.

Acknowledgement. Helpful discussions
gratefully acknowledged. The author
encouragement of Prof. S. Sugiura. Th
preparing the illustrations. The computa
center of Kanazawa University.

References

P. Coppens and W. C. Hamilton (197
Zachariazen approximation. Acta
W. A. Dollase (1967), The crystal struct
from the Steinbach meteorite. Acta
W. A. Dollase and W. H. Baur (1976), T
solved by computer simulation. Ar
W. A. Dollase and M. J. Buerger (1
tridymites. Geol. Soc. Amer. Prog
R. E. Gibbs (1927), The polymorphi
tridymite. Proc. Roy. Soc. **A 113**, 3
W. Hoffmann (1967), Gitterkonstante
Naturwiss. **54**, 114
J. A. Ibers and W. C. Hamilton (1974), I
Vol. IV, Kynoch Press, Birmingha
K. Kato and A. Nukui (1976), Die Kri
Acta Crystallogr. **B 32**, 2486–249
K. Kihara (1977), An orthorhombic s
about 105 and 180° C. Z. Kristallo
A. J. Leadbetter, T. W. Smith, and A. F
Nature Phys. Sci. **244**, 125–126
A. Nukui, H. Nakazawa, and M. Ak
tridymite. In press in Amer. Mine
D. R. Peacor (1973), High temperat
inversion. Z. Kristallogr. **138**, 274
M. Sato (1964), X-ray study of tridymite
J. **4**, 115–130

position is not spherical: the center and its vicinity are negative, but lower positive peaks are tetrahedrally distributed on positions in the other sides of the Si–O bonds. One interpretation is based on assuming that the silicon atoms are relaxed from the correct lattice sites to reduce distortion of tetrahedra. The other is by assuming anharmonic vibrations of the silicon atoms, each of which is in a noncentrosymmetrical field surrounded tetrahedrally by four oxygen atoms. In any event these effects probably contribute to the apparently large thermal motion.

Acknowledgement. Helpful discussions of some points with Dr. T. Matsumoto are gratefully acknowledged. The author would like to acknowledge the continuing encouragement of Prof. S. Sugiura. Thanks are also due to Mr. K. Nakamura for preparing the illustrations. The computations were performed at the data-processing center of Kanazawa University.

References

P. Coppens and W. C. Hamilton (1970), Anisotropic extinction corrections in the Zachariazen approximation. Acta Crystallogr. **A 26**, 71–83

W. A. Dollase (1967), The crystal structure at 220° C of orthorhombic high tridymite from the Steinbach meteorite. Acta Crystallogr. **23**, 617–623

W. A. Dollase and W. H. Baur (1976), The superstructure of meteoritic low tridymite solved by computer simulation. Amer. Mineral. **61**, 971–978

W. A. Dollase and M. J. Buerger (1966), Crystal structure of some meteoritic tridymites. Geol. Soc. Amer. Program 1966, Annual Meeting, 54–55

R. E. Gibbs (1927), The polymorphism of silicon dioxide and the structure of tridymite. Proc. Roy. Soc. **A 113**, 351–368

W. Hoffmann (1967), Gitterkonstanten und Raumgruppe von Tridymit bei 20° C. Naturwiss. **54**, 114

J. A. Ibers and W. C. Hamilton (1974), International tables for X-ray crystallography. Vol. IV, Kynoch Press, Birmingham

K. Kato and A. Nukui (1976), Die Kristallstruktur des monoklinen Tief-Tridymits. Acta Crystallogr. **B 32**, 2486–2491

K. Kihara (1977), An orthorhombic superstructure of tridymite existing between about 105 and 180° C. Z. Kristallogr. **146**, 185–203

A. J. Leadbetter, T. W. Smith, and A. F. Wright (1973), Structure of high cristobalite. Nature Phys. Sci. **244**, 125–126

A. Nukui, H. Nakazawa, and M. Akao (1978), Thermal changes in monoclinic tridymite. In press in Amer. Mineral

D. R. Peacor (1973), High temperature single-crystal study of the cristobalite inversion. Z. Kristallogr. **138**, 274–298

M. Sato (1964), X-ray study of tridymite (1) On tridymite M and tridymite S. Mineral. J. **4**, 115–130